analytical chemistry

pubs.acs.org/ac Article

DNA Conformation-Regulated Hemin Switch for Lab-on-Chip Chemiluminescent Detection of an Antibody Secreted from Hybridoma Cells

Hang Ao,[†] Wencheng Xiao,[†] Wenrui Hu, Jie Wu,* and Huangxian Ju*

Cite This: *Anal. Chem.* 2024, 96, 18502−18509 Read Online

ACCESS | Metrics & More | Article Recommendations | Supporting Information

ABSTRACT: This work designed a DNA conformation-regulated hemin switch for rapid chemiluminescent (CL) detection of a monoclonal antibodies. This switch was performed with an affinity probe and an inhibition probe, which were conveniently prepared by hybridizing hemin-labeled DNA1 with KHL peptide-labeled DNA2 and binding biotin-labeled DNA3 to streptavidin, respectively. In the absence of the target antibody, streptavidin-DNA3 could hybridize with hemin-DNA1/KHL-DNA2 to release KHL-DNA2, which led to the loss of hemin activity due to the affinity hindrance of streptavidin-DNA3. After the KHL peptide was recognized by the target antibody, the strand replacement hybridization could be inhibited by the bound antibody, which retained the high catalytic activity of hemin overhung on the antibody-bound affinity probe for a CL reaction, leading to a "signal-on" process for CL antibody detection. Using a KHL-specific antibody, anti-proprotein convertase subtilisin/kexin type 9 antibody (PCSK9-Ab), as a target model and common L012−1,2,4-triazole−H_2O_2 CL system, the designed switch showed a detection range of 10 ng mL^{-1} to 1 μg mL^{-1} with a detection limit of 4.16 ng mL^{-1} (56.2 pM) and a short analytical time of 6.5 min. The proposed quick method could simply be used for lab-on-chip CL detection of PCSK9-Ab in situ-secreted from PCSK9-6E3 hybridoma cells, which showed an accuracy of 90.2% compared with the statistical results from general fluorescence imaging, providing a potential technique for screening specific hybridoma cells.

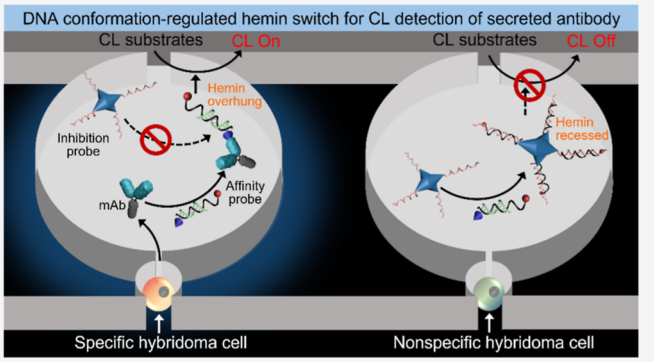

Downloaded via NANJING UNIV on November 26, 2024 at 15:51:15 (UTC).
See https://pubs.acs.org/sharingguidelines for options on how to legitimately share published articles.

The production of monoclonal antibody drugs has been developing rapidly since the first introduction of hybridoma technology in 1975, which promotes the quick development of immunotherapy strategies in oncology.[1−3] The screening of hybridoma cells with a high secretory capacity is a key step in hybridoma technology. Enzyme-linked immunosorbent assay is the primary method for screening specific hybridoma cells. However, the time-consuming cell culture, complex detection procedure including multiple washing, and low sensitivity hinder the production efficiency of monoclonal antibodies.[4,5] A series of single-cell screening assays have been established based on the detection of cell-secreted specific proteins, and the in situ detection of single hybridoma cell-secreted antibodies on a microfluidic chip has become an efficient technology to improve the efficiency of hybridoma cell screening.[6−8] By isolating a single hybridoma cell in a microdroplet or microchamber, the in situ-secreted antibody can be detected in a restricted atmosphere, and specific hybridoma cells can be sorted by flow cytometry. Based on those single-cell technologies for rapid analysis of hybridoma cells and specific detection of antibodies, fast monoclonal antibody discovery for emergency treatment, such as SARS-CoV-2, has been developed.[9−12] However, these developed fluorescence (FL) and colorimetric microdroplet-based chip screening methods are usually limited due to the lack of a one-step homogeneous probe for antibody detection, which is unfavorable to extending hybridoma cell screening on microchips. Besides, long-term incubation of hybridoma cells in a microatmosphere might reduce the activity of hybridoma cells.[13] Therefore, it is necessary to develop a universal and rapid assay for the detection of hybridoma cell-secreted antibodies.

Chemiluminescence (CL) assays have occupied a very large proportion of clinical applications in biochemical detection due to its cost-effectiveness and high sensitivity,[14−16] and the CL immunoassay (CLIA) has provided an effective way for protein detection. However, the conventional heterogeneous CLIA suffers from the drawbacks of tedious assay time, complex washing steps, and the requirement of skilled operators. Thus,

Received: August 5, 2024
Revised: October 21, 2024
Accepted: October 25, 2024
Published: November 6, 2024

ACS Publications © 2024 American Chemical Society

Scheme 1. Schematic Diagram of DNA Conformation-Regulated Hemin Switch Controlled by Immuno-Mediated Steric Hindrance for the CL Assay of the Target Antibody[a]

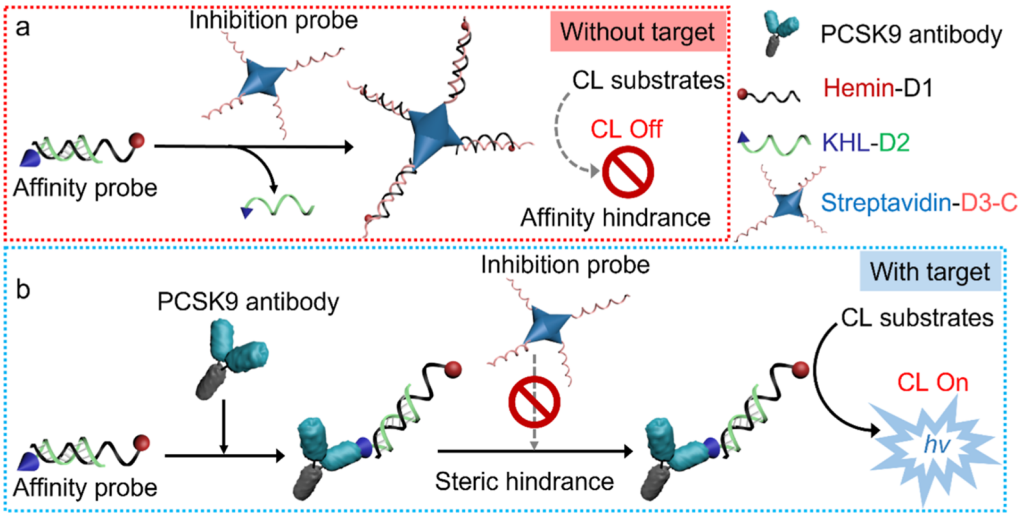

[a]Illustration of the reaction between the affinity probe and inhibition probe in the absence (a) and presence (b) of the PCSK9 antibody.

homogeneous CLIA is more favored in clinical detection nowadays, which provides the possibility of developing rapid, convenient, and sensitive assays for protein biomarkers due to the elimination of complex operation and washing steps. Additionally, a homogeneous solution provides a more native reaction environment for protein recognition, which can prevent the conformational changes of proteins in nonnative surfaces and thus further improve the assay accuracy.[17] The construction of the CL switch is the primary and most important step for the homogeneous CL assay. Compared to complex and costly split luciferase systems,[18,19] enzyme mimic DNAzyme-based switches are more favored in homogeneous CL assays.[20] By composing hemin and a G-rich DNA sequence to form a G-quadruplex DNA structure with peroxidase activity, the G4/hemin can generate a strong CL signal with CL substrates.[21−23] Unfortunately, the utilization of G4/hemin-based CL switch is primarily limited in laboratory settings due to the poor solubility of hemin and its self-aggregation to inactive dimers in aqueous solution.[24,25]

The utilization of the hemin−oligonucleotide complex not only improves the solubility and stability of hemin but also eliminates the restriction of DNA sequence in the G4/hemin system. Ju and co-workers reported previously a dual-hemin-labeled DNA switch for homogeneous FL detection of DNA.[26] After recognition of the target sequence, the conformation of the hemin moiety changed from dimer into monomer, resulting in the increased peroxidase activity of hemin moiety to generate an enhanced fluorescent signal. Additionally, a strand displacement-activated double-stranded hemin−DNA switch was also designed for DNA sensing.[27] Subsequently, Cheng and co-workers utilized hemin−DNA to establish a proximity-induced assembly of zippered G4/hemin for colorimetric detection of target DNA and fluorescent imaging of protein dimerization on cell surfaces by proximity-activated tyramide signal amplification.[28] These hemin−DNA complexes exhibit their great potential in developing homogeneous CL switches.

In this work, a novel DNA conformation-regulated hemin switch was designed for fast CL detection of monoclonal antibodies with an affinity probe and an inhibition probe. The affinity probe could be conveniently prepared by hybridizing hemin-labeled DNA1 with KHL peptide-labeled DNA2 to overhang the hemin at the end of the DNA strand for catalyzing the CL reaction of common L012−1,2,4-triazole−H_2O_2 CL systems. After the affinity probe was incubated with an inhibition probe, streptavidin−DNA3, their strand replacement hybridization (SRH) greatly reduced the peroxidase activity of the hemin due to its recess (Scheme 1a). In the presence of a KHL-specific target antibody, the immunological recognition led to a steric hindrance to the SRH of the affinity probe with the inhibition probe, thus retaining the high catalytic activity of overhung hemin to achieve a "signal-on" CL process (Scheme 1b). Using antiproprotein convertase subtilisin/kexin type 9 antibody (PCSK9-Ab) as a target model, the proposed CL assay showed excellent performance along with an analytical time of 6.5 min, including two-step incubations with the target antibody and then the inhibition probe. The quick method resulted in its promising application in lab-on-chip CL detection of PCSK9-Ab in situ-secreted from PCSK9-6E3 hybridoma cells and provided a potential technique for screening the specific hybridoma cells.

EXPERIMENTAL SECTION

Reagents and Materials. Sodium ascorbate, $CuSO_4$, sodium acetate, ethanol, isopropyl alcohol, 1*H*-1,2,3-triazole-1-acetic acid (BTTAA), K_2HPO_4, KH_2PO_4, 1,2,4-triazole (Tz), luminol, *N*-(4-aminobutyl)-*N*ethylisoluminol (ABEI), 3,3′,5,5′-tetramethylbenzidine dihydrochloride, and SYLGARD 184 silicone elastomer kit containing polydimethylsiloxane and curing agent were purchased from Sigma-Aldrich Co. (Shanghai, China). Streptavidin was purchased from Aladdin Biochemical Technology Co., Ltd. (Shanghai, China). CellTracker Red CMTPX dye was purchased from Yeasen Biotechnology (Shanghai) Co., Ltd. 8-Amino-5-chloro-2,3-dihydro-7-phenylpyrido-(3,4-d)-pyridazine-1,4-dione (L012) was purchased from Wako Pure Chemical Industries, Ltd. (Osaka, Japan). Isoluminol was purchased from Meryer Biochemical Technology (Shanghai, China). Silicon wafer, photoresist SU8-3025, and its developer were obtained from MicroChem Co., Ltd. (USA). Fetal bovine serum (FBS),

https://doi.org/10.1021/acs.analchem.4c04122
Anal. Chem. 2024, 96, 18502−18509

HEPES buffer, sodium pyruvate, L-glutamine, and PS solution (10 U mL^{-1} penicillin and 10 mg mL^{-1} streptomycin) were purchased from Thermo Fisher (Shanghai, China). Anti-α-fetoprotein antibody (AFP-Ab, mouse monoclonal antibodies, clone nos. 9K5) and anticarcinoembryonic antigen−antibody (CEA-Ab, mouse monoclonal antibodies, clone nos. 2H4) were purchased from Beijing Key-biotech Co. Ltd. (China). Anti-proprotein convertase subtilisin/kexin type 9 antibody (PCSK9-Ab, mouse monoclonal antibodies, clone nos. 6E3), PCSK9-6E3 hybridoma cells, anti-amino-terminal pro-brain natriuretic peptide antibody (NT-proBNP-Ab, mouse monoclonal antibodies, clone nos. T6) and anti-SARS-CoV-2 nucleocapsid protein antibody (SARS-CoV-2 NP-Ab, mouse monoclonal antibodies, clone nos. 8B1) were supplied by FANTIBODY (Chongqing, China). Dulbecco's modified Eagle medium (DMEM) was obtained from KeyGEN BioTECH Corp. Ltd. (Jiangsu, China). Hemin-labeled oligonucleotides were purchased from Takara Bio Inc. (Beijing, China). Hydrogen peroxide (30%) and alkynyl-modified PCSK9 peptide NH_2-L-propargylglycine-EGRVMVTDFENV-PEEDGTRFHRQAS (alkynyl-KHL) and other DNA oligonucleotides were obtained from Sangon Biotechnology Co. Ltd. (Shanghai, China). The DNA sequences are listed in Table S1. Ultrapure water from a Millipore water purification system (Milli-Q, Millipore) was used for all of the experiments.

Apparatus. The CL imaging of the microfluidic chip was performed in a Tanon 5200 multi-automatic CL image analysis system, and other CL imaging measurements were conducted with a BioSpectrum 615 imaging system. The CL signal was processed by VisionWorks, and the CL intensity was collected by the mean pixel intensity within a circle. CL kinetic curves were obtained on MPI-A multifunctional electrochemical and CL analytical system with PMT 400 (Xi'an Remex Analytical Instrument Co., Ltd. China). Circular dichroism (CD) spectra were collected by a MOS-500 circular dichroism spectrometer (Applied Photophysics Ltd., UK). Absorption spectra were recorded on a UV-3600 UV−vis−NIR spectrophotometer (Shimadzu Company, Japan). Photolithography was carried out on a pattern conversion and nano-imprint system (SUSS, Germany). Oxygen plasma treatments of glass and PDMS were conducted with a plasma cleaner PDC-002 (Harrick, USA). A Leica microscope was used for the bright field and FL imaging on a microfluidic chip, and the wide images of the microfluidic chip were obtained through image stitching with an electric stage.

Preparation of KHL-D2. KHL-modified DNA2 (KHL-D2) was synthesized through the click reaction between azide-modified D2 (N_3-D2) and alkynyl-KHL. Briefly, $CuSO_4$ (10 μL, 100 μM) and BTTAA (60 μL, 10 mM) were first mixed, and 10 μL of a freshly prepared sodium ascorbate solution (50 mM) was then added to the mixture. After vigorous stirring for a few seconds, N_3-D2 and alkynyl-KHL were successively added to adjust the volume to 100 μL with ultrapure water. Then, the mixture was incubated overnight at 37 °C. It was followed by the addition of sodium acetate (10 μL, 3 M) into the mixture and stirring for 5 min (200 rpm), and 200 μL of cold ethanol was then added to purify the produced KHL-D2. After 1 h of aging at −20 °C, 10 min centrifugation at 12,000 rpm, and 10 min centrifugal washing with 70% cold ethanol at 12,000 rpm 3 times, a white solid product was obtained and it was redissolved in PBS (pH 7.4, 10 mM).

Preparation of the Affinity Probe and Inhibition Probe. The affinity probe (hemin-D1/D2-KHL) was obtained by mixing KHL-D2 and hemin-D1 in a ratio of 1:1 to react at 37 °C for 30 min. The inhibition probe (SA-D3-C) was obtained by mixing SA and biotin-T-D3-C in a ratio of 1:4 to react at 37 °C for 1 h. The synthesized probes were stored at 4 °C for further use.

CL Detection of PCSK9-Ab. Then, 26 μL of PCSK9-Ab or the sample was mixed with hemin-D1/D2-KHL (1 μL, 1 μM) and incubated for 5 min; 1 μL of SA-D3-C (2.5 μM) was added to incubate for 1 min. The reaction solution was mixed with 22 μL of a CL substrate containing L012 (10 μL, 1 mM), Tz (2 μL, 200 mM), and H_2O_2 (10 μL, 2 mM) to collect the CL signal with an exposure time of 30 s.

Measurement of Catalytic Activity. A CL method was used to evaluate the activity of hemin-D1/D2 or hemin-D1/D3-C in the L012−Tz−H_2O_2 system. The time-dependent CL intensity was immediately collected after the injection of different concentrations of L012 into 10 mM PBS (pH 7.2) containing 20 nM hemin-D1/D2 (or hemin-D1/D3-C), 0.4 mM H_2O_2, and 4 mM Tz. The initial rate (V_0) in the presence of hemin-D1/D2 or hemin-D1/D3-C was gained from the slope of the plot of the maximum CL intensity vs the corresponding reaction time. The Lineweaver−Burk plot was used to calculate the Michaelis constant K_m and the maximum reaction rate V_{max}.

Electrophoresis Analysis. 8% native polyacrylamide gel was prepared using 1× TBE buffer to load the mixtures, which were prepared by mixing 4 μL samples with 1 μL of 6× loading buffer and 1 μL of SYBRGold dye to stand for 3 min. Gel electrophoresis was run at 100 V for 30 min in 1× TBE buffer and visualized by a BioSpectrum 615 imaging system.

Chip Fabrication. After solidifying the photoresist at a 25 μm height on a silicon wafer, a mask with the designed structure was covered on the wafer for 4.5 s of exposure under ultraviolet light in a photoetching machine. This wafer was then baked at 90 °C for 30 min to fix the photolithographic structure. After alternately developing in a developer and isopropanol to remove the excess photoresist, the designed structure was obtained by heating the silicon wafer at 180 °C for 30 min.

A PDMS precursor solution was prepared by thoroughly stirring the mixture of polydimethylsiloxane and the curing agent at a ratio of 10:1, in which the bubbles were removed with a pump. The silicon wafer with the formed structure was then immersed in the PDMS precursor solution to cure at 85 °C for 30 min. The resulting PDMS pattern was peeled off of the silicon wafer. Holes with a 1.5 mm diameter were punched on the PDMS structure for inlets and outlets. The chip was finally fabricated by bonding the PDMS on glass (2.5 × 4.0 cm) after oxygen plasma treatment and immersed in 1× PBS before use.

Assay of PCSK9-Ab on the Chip. After the PCSK9-Ab sample was diluted with DMEM, 1 μL of hemin-D1/D2-KHL (1 μM) was first mixed with 26 μL of the PCSK9-Ab sample and injected into the microchip immediately, which formed droplets in the microwells through air injection. After 5 min of incubation, 5 μL of SA-D3-C (0.5 μM) was injected into the microchip for 1 min of incubation. Then, 22 μL of the CL substrate containing L012 (10 μL, 1 mM), Tz (2 μL, 100 mM), and H_2O_2 (10 μL, 2 mM) was injected into the microchip to collect the CL image by a CCD with an exposure time of 1.5 min.

In Situ Detection of PCSK9-Ab Secreted from Hybridoma Cells. PCSK9-6E3 hybridoma cells were first

https://doi.org/10.1021/acs.analchem.4c04122
Anal. Chem. 2024, 96, 18502−18509

cultured in DMEM supplemented with 20% FBS, 0.1 mg mL^{-1} streptomycin, and 0.1 mg mL^{-1} penicillin at 37 °C and 5% CO_2. After gently washing with PBS 8 times, they were directly blown off with a pipet and resuspended in PBS. Then, the cell suspension (2.37×10^4 cell mL^{-1}) was injected into the PBS-presoaked microchip. After the hybridoma cells captured in the microwells were cultured for 10 min to adhere in a microchip, DMEM containing hemin-D1/D2-KHL (20 nM) was injected into the chip to replace PBS and form droplets in the microwells through air injection. The microchip was finally incubated for 1 h to secrete the specific antibody, which was detected by injecting SA-D3-C (5 μL, 0.5 μM) into the microchip to incubate for 1 min and then 22 μL of the CL substrate to collect the CL image by a CCD with an exposure time of 1.5 min.

To confirm the proposed detection method for PCSK9-Ab secreted from specific hybridoma cells, the captured PCSK9-6E3 hybridoma cells were stained with CellTracker Red CMFDA to perform general FL imaging for statistical analysis.

RESULTS AND DISCUSSION

DNA Conformation-Regulated Hemin Switch. Figure 1a illustrates the principle of a DNA conformation-regulated hemin switch. A strong CL signal can be produced by the catalysis of the hemin moiety overhung at the end of the D1 strand of hemin-D1/D2 to the CL reaction. After the hemin-D1 is hybridized with the D3-C sequence longer than D1, the hemin moiety in hemin-D1 is recessed in a double-stranded DNA structure (dsDNA), which reduces the peroxidase activity of the hemin moiety and leads to a CL "signal off" state. This conformation-regulated hemin switch was demonstrated by detecting the CL intensity of different emitters[29] in 10 mM pH 7.2 PBS containing Tz, H_2O_2, and hemin-D1, hemin-D1/D2, or hemin-D1/D3-C (Figure 1b). The results indicated that L012 was the most sensitive CL emitter; thus, it was used for the following experiments.

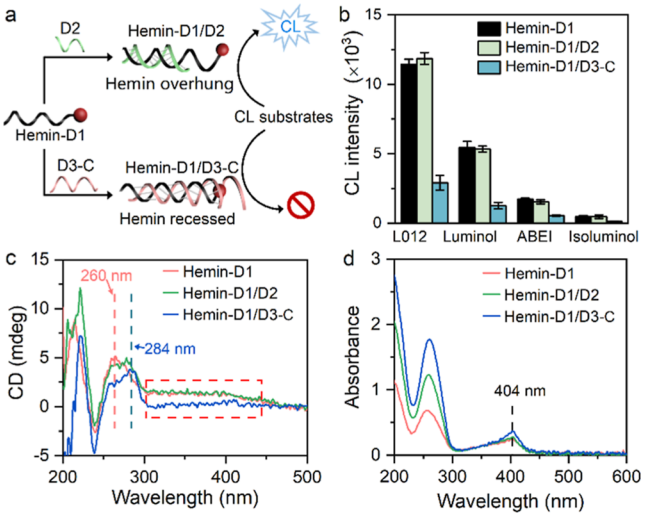

Figure 1. (a) Principle of DNA conformation-regulated hemin switch. (b) CL intensity of 10 mM pH 7.2 PBS containing 4 mM Tz, 0.4 mM H_2O_2, 20 nM hemin-D1, hemin-D1/D2 or hemin-D1/D3-C, and 0.2 mM emitter L012, luminol, ABEI, or isoluminol. (c,d) CD (c) and UV−vis (d) spectra of 5 μM hemin-D1, hemin-D1/D2, and hemin-D1/D3-C in 10 mM pH 7.2 PBS.

To gain more insights into the DNA conformation-regulated hemin switch, the conformation change of the hemin moiety was confirmed by CD measurements (Figure 1c). The hemin-D1 showed a CD absorption peak at 260 nm and a broad CD absorption band from 300 to 450 nm, which were attributed to the single-strand DNA and the Soret region of the hemin moiety,[30] respectively. After the hybridization of hemin-D1 to D2 or D3-C, the CD absorption peak at 260 nm shifted to 284 nm,[31] while the broad CD absorption band disappeared, which implied the conformation change of the hemin moiety. A similar phenomenon was also observed in the UV−vis absorption spectra (Figure 1d). The hemin absorption peak at 404 nm rose only when the hemin moiety was recessed in the dsDNA, which could be attributed to the hyperchromic effect caused by the proximity of DNA bases to the porphyrin of hemin.[32,33] Besides, the kinetic curves of hemin-D1/D2 and hemin-D1/D3-C with different concentrations of L012 were recorded to measure the K_m and V_{max} values (Table S2). The K_m value of hemin-D1/D3-C was found to be higher than that of hemin-D1/D2, indicating the affinity decrease of L012 to the hemin moiety,[34] which led to a lower enzymatic reaction rate.

The designed homogeneous switch is different from other hemin-based switches reported previously. The general G4/hemin-based switch is based on the stability improvement of the hemin monomer upon binding to a specific DNA sequence (Figure S1), which enhances the hemin activity. The strand displacement-activated double-stranded hemin−DNA switch is based on the dissociation of the hemin dimer labeled at two complementary DNA strands, which is triggered by the target DNA. Herein, the proposed hemin-based switch is performed through the affinity regulation of the hemin moiety upon the conformation change of the hemin moiety, which greatly enhances the flexibility in the application of the homogeneous peroxidase activity switch.

Immuno-Mediated Steric Hindrance for the CL Assay of the PCSK9 Antibody. To detect PCSK9-Ab, the KHL peptide, which can be specifically recognized by PCSK9-Ab, was labeled to DNA2, and the KHL-D2 was used to prepare the affinity probe of PCSK9-Ab. The successful synthesis of KHL-D2 through the click reaction between azide-modified D2 and alkyne-modified KHL was confirmed by PAGE (Figure S2), which exhibited a slower migration due to the higher molecule weight of KHL-D2 (line 4) than pure D2 (line 2). The affinity probe hemin-D1/D2-KHL was constructed by the hybridization of hemin-D1 and KHL-D2, which formed a steric hindrance regulation region at the 3′-end for target protein recognition and a hemin activity regulation region at 5′-end for signal production (Figure 2a). After PCSK9-Ab was recognized by the KHL, the inhibition probe, which contained a large protein molecule at the 5′-end of D3-C, could not hybridize with hemin-D1 in the affinity probe to replace KHL-D2 due to the formed steric hindrance between PCKS9-Ab-bonded KHL-D2 and streptavidin-bonded D3-C, thus keeping the high enzymatic activity of the affinity probe for CL detection of PCSK9-Ab (Scheme 1b).

In order to get the best performance of the DNA conformation-regulated hemin switch, the sequences of D1, D2, and D3 were optimized due to the crucial effect of the nucleobase modification on hemin catalytic capacity.[27,35] The hemin−DNA with different adjacent bases in the hemin binding site was first assessed. All hemin-D1 variants exhibited an obvious signal decrease when the hemin moiety was

https://doi.org/10.1021/acs.analchem.4c04122
Anal. Chem. 2024, 96, 18502−18509

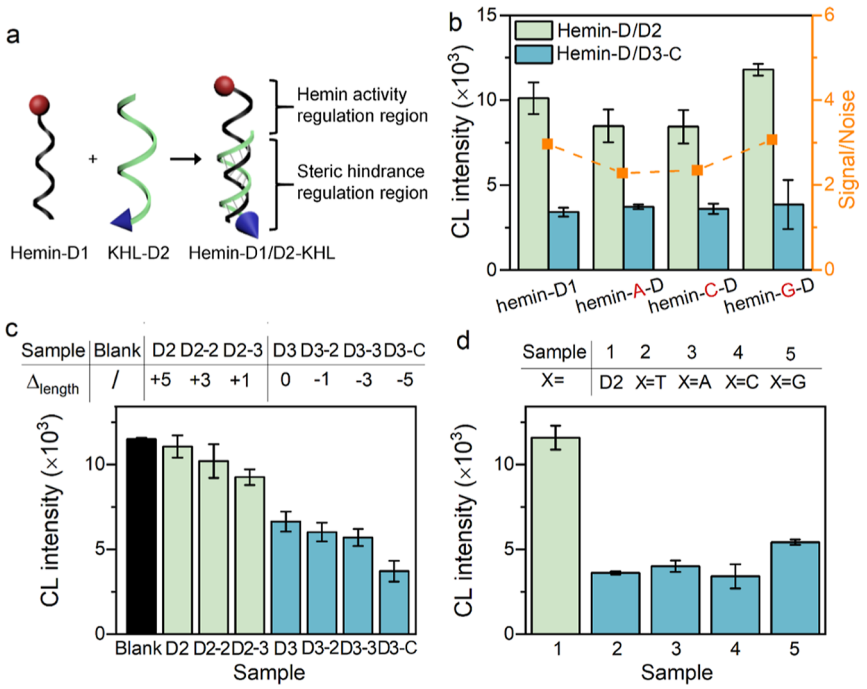

Figure 2. (a) Schematic diagram of preparation of the affinity probe (hemin-D1/D2-KHL). (b) Optimization of the adjacent base bound with the hemin moiety. (c) Optimization of the length of D2 and D3, Δ_{length} = the more base number of D1 than D2 (or D3). (d) Effect of terminal bases of 3′-XXXXX-D3-5′ to CL intensity.

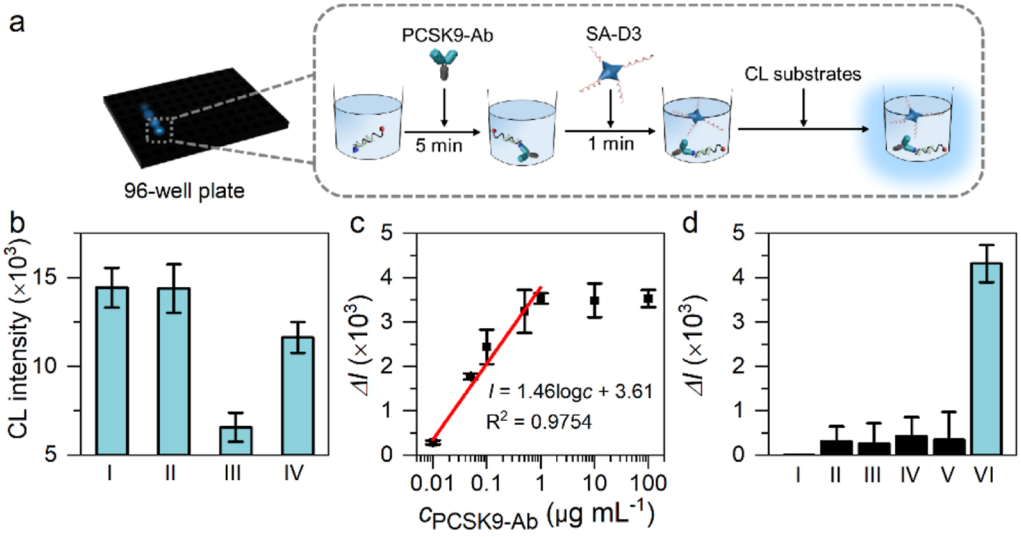

Figure 3. (a) Schematic diagram of CL detection of PCSK9-Ab on a 96-well plate with the DNA conformation-regulated hemin switch. (b) CL intensity of 10 mM pH 7.2 PBS containing 4 mM Tz, 0.2 mM L012, 0.4 mM H_2O_2, and 20 nM hemin-D1/D2-KHL in the absence (I) and presence of 1 μg mL^{-1} PCSK9-Ab (II) or 50 nM SA-D3 (III) after 5 min of incubation and (II) after further incubation with 50 nM SA-D3-C for 1 min (IV). (c) Plot of the relative CL signal vs PCSK9-Ab concentration. (d) CL responses to PBS (I), 1 μg mL^{-1} CEA-Ab (II), AFP-Ab (III), SARS-CoV-2 NP-Ab (IV), NT-proBNP-Ab (V), and PCSK9-Ab (VI).

changed from the overhung to the recessed state (Figure 2b), which demonstrated the flexibility and universality of the proposed DNA conformation-regulated hemin switch. Considering the maximum signal-to-noise ratio, hemin-D1 was selected for further application.

The lengths of D2 and D3, which hybridized with hemin-D1 were found to be the primary factor to affect the performance of the proposed DNA conformation-regulated hemin switch. When the hemin moiety was overhung at the end of the hemin-D1/D2 duplex with 5 uncomplementary bases, the CL signal did not change (Figure 2c), where the length of D2 was 22 bases. However, the CL signal decreased with the increasing number of complementary bases due to the flexibility reduction of the hemin moiety at the end of hemin-D1, and the lowest CL signal was obtained when D3-C (32 bases) had 5 bases longer than hemin-D1. Therefore, D2 with 22 bases and D3-C with 32 bases were selected for the preparation of the affinity probe hemin-D1/D2-KHL and inhibition probe SA-D3-C. In addition, the terminal bases modified at the 3′ end of D3 were also optimized, and D3-C was chosen for the synthesis of inhibition probe SA-D3-C (Figure 2d).

https://doi.org/10.1021/acs.analchem.4c04122
Anal. Chem. 2024, 96, 18502−18509

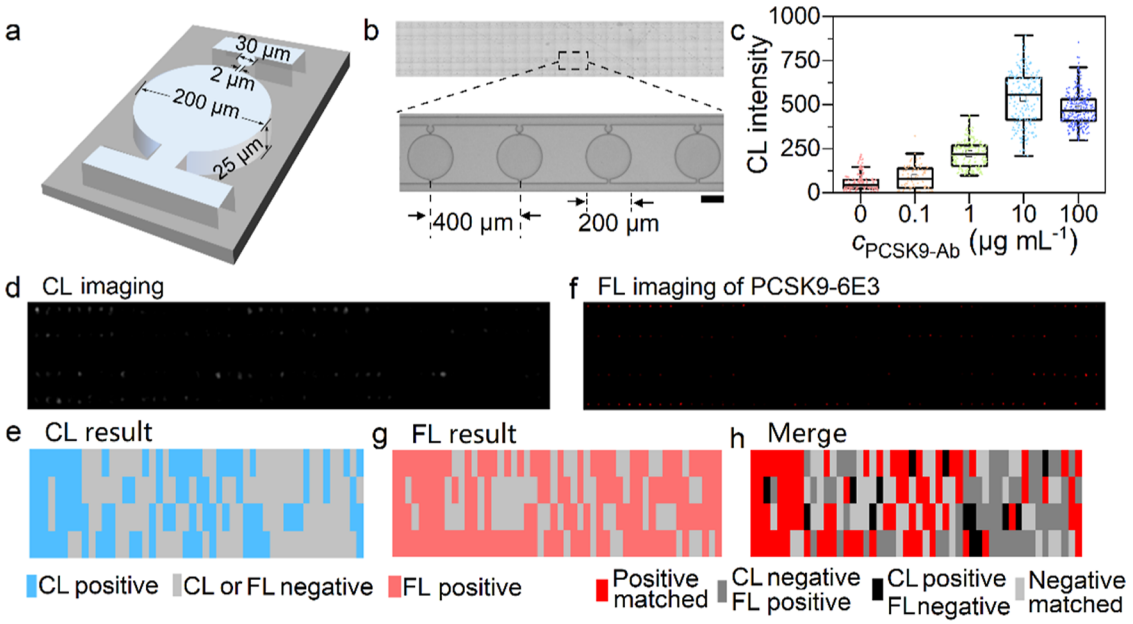

Figure 4. (a) 3D cartoon diagram of the CL imaging unit on the chip with marked size. (b) Bright-field image of the designed microchip. The scale bar is 100 μm. (c) CL intensity of DMEM containing 4 mM Tz, 0.2 mM L012, 0.4 mM H_2O_2, 50 nM SA-D3, 20 nM hemin-D1/D2-KHL, and different concentrations of PCSK9-Ab. (d) CL imaging for detection of secreted PCSK9-Ab from PCSK9-6E3 hybridoma cells on chip, (e) FL imaging of loaded PCSK9-6E3 hybridoma cells. (f) CL statistical result of (d), (g) FL statistical result of the (e,h) corresponding comparison result of (f,g).

Besides, detection conditions including pH, concentration of Tz, L012, and H_2O_2 were also optimized. With the increasing pH of the detection solution, the CL signal increased and the maximum signal-to-noise ratio appeared at pH 7.2 (Figure S3a), which was the physiological pH for guaranteeing the activity of the target antibody and hybridoma cells. Thus, the following measurements were performed at pH 7.2. Besides, the CL signal increased with an increasing concentration of CL enhancer Tz (Figure S3b). Considering the maximum signal-to-noise ratio, 4 mM Tz was selected. Similarly, the optimal concentrations of L012 and H_2O_2 were 0.2 and 0.4 mM, respectively (Figure S3c,d).

The concentration of the inhibition probe SA-D3-C and the incubation time for immune recognition and inhibition were further optimized. When 20 nM hemin-D1/D2-KHL was used for PCSK9-Ab detection, the CL signal reached the lowest intensity when the concentration of SA-D3 was 50 nM (Figure S4), which was used for antibody detection. The addition of SA-D3 resulted in an obvious decrease of the CL signal with only 1 min of incubation (Figure S5a), and a 5 min incubation was sufficient for the immune recognition of PCSK9-Ab to affinity probe hemin-D1/D2-KHL (Figure S5b). Therefore, the entire detection procedure only required a total incubation time of 6 min.

A simple workflow for PCSK9-Ab detection was illustrated in Figure 3a. PCSK9-Ab was first incubated with the affinity probe hemin-D1/D2-KHL for 5 min, and SA-D3-C was then added for 1 min incubation. Afterward, the CL substrate was added for CL imaging. Interestingly, the addition of PCSK9-Ab did not affect the CL signal of the affinity probe (Figure 3b, column II), while a sharp CL decrease was observed when SA-D3-C was mixed with the hemin-D1/D2-KHL (Figure 3b, column III). However, the CL signal of hemin-D1/D2-KHL could be maintained in the presence of PCSK9-Ab (Figure 3b, column IV), which demonstrated the feasibility of the proposed CL assay for the target antibody based on the DNA conformation-regulated hemin switch controlled by immuno-mediated steric hindrance.

Under the optimized conditions, a concentration-dependent CL response to PCSK9-Ab was observed. The proposed CL assay achieved PCSK9-Ab detection in the range from 10 ng mL^{-1} to 1 μg mL^{-1} with a detection limit of 4.16 ng mL^{-1} (56.2 pM) at 3 times standard deviation (Figure 3c), which was at least 2 orders of magnitude lower than other rapid assays for antibodies without amplification, including heterogeneous electrochemical assays (10 nM)[36−38] and the homogeneous FL assay (5.6,[39] 3,[40] and 1 nM[41]). Besides, the specificity of the proposed CL assay was also evaluated by detecting different proteins, and no obvious CL signal was observed except PCSK9-Ab, indicating the good selectivity of the proposed CL assay (Figure 3d).

Lab-on-Chip Detection of PCSK9-Ab. The designed microfluidic chip contained 200 microwells (50 units × 4 rows) for antibody detection secreted from single cells (Figure S6) via in situ CL imaging. The single-cell detection unit was composed of a single-cell capture site and a CL reaction chamber (Figure 4a), and a single hybridoma cell could be captured through the differential flow resistance principle.[42−44]

In order to obtain a CL image with a clear shape of the CL dot signal and avoid the signal interference on the microchip, which was caused by the scattering CL signal, each CL reaction chamber had a diameter of 200 μm, and the spacing between each unit was 400 μm (Figure 4b). Upon injections of the mixture of the diluted PCSK9-Ab sample, hemin-D1/D2-KHL, SA-D3-C, and then the CL substrate into the microwells on the microfluidic chip, a concentration-dependent CL response was observed similar to the above assay with 96-well plates. The CL intensity increased with the increasing concentration of PCSK9-Ab and reached the highest value at a concentration of 10 μg mL^{-1} (Figure 4c). Considering the high local

https://doi.org/10.1021/acs.analchem.4c04122
Anal. Chem. 2024, 96, 18502−18509

concentration of the target antibody in situ-secreted from single hybridoma cells in the confined microchamber,[7,10] the proposed CL assay was supposed for lab-on-chip detection of the antibody secreted from single hybridoma cells.

CL Detection of the Antibody Secreted from PCSK9-6E3 Hybridoma Cells. The cellular toxicity of two probes and the CL substrate was first evaluated. Long-term incubation of hybridoma cells with affinity probe hemin-D1/D2-KHL did not change their viability (Figure S7a), and a 10 min incubation, longer than the detection application, of the hybridoma cells with both SA-D3-C and the CL substrate also did not show obvious viability decrease (Figure S7b), indicating the good biocompatibility of these designed probes and detection reagents.

After the suspension of PCSK9-6E3 hybridoma cells (2.37×10^4 cell mL^{-1}) was injected into the microchip, which was presoaked in PBS to prevent the solution absorption by PDMS, a single hybridoma cell could be well captured in each capture site. The bright-field image showed that the microchip with 200 microwells captured 148 cells (Figure S8). After these cells were incubated with DMEM containing hemin-D1/D2-KHL for 1 h to secrete the specific antibody, the CL imaging of the secreted PCSK9-Ab was performed (Figure 4d). The CL image showed 91 positive PCSK9-6E3 hybridoma cells, which could quickly secrete PCSK9-Ab for CL detection (Figure 4e). In order to confirm the accuracy of the proposed CL assay, the captured PCSK9-6E3 hybridoma cells were further stained with CellTracker Red CMFDA dye, and their positions were observed by general FL imaging (Figure 4f). From the FL image, 148 captured cells could be observed (Figure 4g). After merging the CL and FL images, it was found that 14 positions showed negative FL but positive CL, which could be considered as false positive due to the operation error caused by the leakage of secreted PCSK9-Ab during the injections of inhibition probe SA-D3-C and the CL substrate to the microwells. Thus, the accuracy of the proposed CL assay was calculated to be 90.2%. In fact, the operation error could be decreased by a skilled operator to further enhance the accuracy. The attractive advantages of the DNA conformation-regulated hemin switch-based CL assay, such as rapidity, simplicity, and good accuracy, indicated that the proposed CL assay possessed a promising application in lab-on-chip CL detection of PCSK9-Ab in situ-secreted from PCSK9-6E3 hybridoma cells and provided a potential technique for screening the specific hybridoma cells.

CONCLUSIONS

A DNA conformation-regulated hemin switch was designed as a novel type of hemin-based switch for rapid CL detection of PCSK9-Ab. This switch was performed with an affinity probe hemin-D1/D2-KHL and an inhibition probe SA-D3-C used to regulate the catalytic activity of hemin moiety at the 5′-end of D1. The peroxidase activity regulation of the overhung hemin moiety on the affinity probe could be conveniently achieved through the SRH between the affinity probe and inhibition probe to form the recessed hemin moiety, which greatly depended on the steric hindrance resulting from the immunological recognition of target PCSK9-Ab to KHL at 5′-end of D2. With the optimized sequences of D1, D2, and D3, times for recognition reactions, and CL detection conditions, the proposed CL assay showed excellent performance along with an analytical time of 6.5 min, including the two-step recognition, which led to a promising technique for lab-on-chip CL detection of antibody secreted from hybridoma cells and screening of the specific hybridoma cells.

ASSOCIATED CONTENT

Supporting Information

The Supporting Information is available free of charge at https://pubs.acs.org/doi/10.1021/acs.analchem.4c04122.

Oligonucleotide sequences; kinetic parameter comparison; schematic diagram of three types of hemin-based CL switches; gel electrophoresis analysis of KHL-D2; optimization of CL detection conditions; SA-D3-C concentration and incubation time; CAD design of microchips; CCK-8 results of hybridoma cells; and bright-field image of captured single hybridoma cells in microchips (PDF)

AUTHOR INFORMATION

Corresponding Authors

Jie Wu − *State Key Laboratory of Analytical Chemistry for Life Science, School of Chemistry and Chemical Engineering, Nanjing University, Nanjing 210023, China;* orcid.org/0000-0003-1379-122X; Phone: +86-25-89683593; Email: wujie@nju.edu.cn

Huangxian Ju − *State Key Laboratory of Analytical Chemistry for Life Science, School of Chemistry and Chemical Engineering, Nanjing University, Nanjing 210023, China;* orcid.org/0000-0002-6741-5302; Email: hxju@nju.edu.cn

Authors

Hang Ao − *State Key Laboratory of Analytical Chemistry for Life Science, School of Chemistry and Chemical Engineering, Nanjing University, Nanjing 210023, China*

Wencheng Xiao − *State Key Laboratory of Analytical Chemistry for Life Science, School of Chemistry and Chemical Engineering, Nanjing University, Nanjing 210023, China*

Wenrui Hu − *State Key Laboratory of Analytical Chemistry for Life Science, School of Chemistry and Chemical Engineering, Nanjing University, Nanjing 210023, China*

Complete contact information is available at: https://pubs.acs.org/10.1021/acs.analchem.4c04122

Author Contributions

†H.A. and W.X. contributed equally. All authors have approved the final version of the manuscript.

Notes

The authors declare no competing financial interest.

ACKNOWLEDGMENTS

This work was financially supported by the National Natural Science Foundation of China (21827812, 21635005, and 21890741) and the Independent Research Foundation from the State Key Laboratory of Analytical Chemistry for Life Science (5431ZZXM24010).

REFERENCES

(1) Köhler, G.; Milstein, C. *Nature* **1975**, *256*, 495−497.
(2) Beck, A.; Wurch, T.; Bailly, C.; Corvaia, N. *Nat. Rev. Immunol.* **2010**, *10*, 345−352.
(3) Dumontet, C.; Reicher, J. M.; Senter, P. D.; Lambert, J. M.; Beck, A. *Nat. Rev. Drug Discovery* **2023**, *22*, 641−661.

(4) Zhang, C. In *Methods in Molecular Biology: Antibody Methods and Protocols*; Proetzel, G., Ebersbach, H., Eds.; Springer: Totowa, 2012; pp 117−135.
(5) Zhang, D.; Xie, C. J.; Wang, R. Z.; Yang, Q. H.; Chen, H. L.; Ling, S. M.; Wang, S. H.; Jia, K. Z. *BMC Biotechnol.* **2018**, *18*, 25−34.
(6) Theberge, A. B.; Courtois, F.; Schaerli, Y.; Fischlechner, M.; Abell, C.; Hollfelder, F.; Huck, W. T. S. *Angew. Chem., Int. Ed.* **2010**, *49*, 5846−5868.
(7) Debs, B. E.; Utharala, R.; Balyasnikova, I. V.; Griffiths, A. D.; Merten, C. A. *Proc. Natl. Acad. Sci. U.S.A.* **2012**, *109*, 11570−11575.
(8) Armbrecht, L.; Dittrich, P. S. *Anal. Chem.* **2017**, *89*, 2−21.
(9) Mazutis, L.; Gilbert, J.; Ung, W. L.; Weitz, D. A.; Griffiths, A. D.; Heyman, J. A. *Nat. Protoc.* **2013**, *8*, 870−891.
(10) Eyer, K.; Doineau, R. C. L.; Castrillon, C. E.; Briseño-Roa, L.; Menrath, V.; Mottet, G.; England, P.; Godina, A.; Brient-Litzler, E.; Nizak, C.; Jensen, A.; Griffiths, A. D.; Bibette, J.; Bruhns, P.; Baudry, J. *Nat. Biotechnol.* **2017**, *35*, 977−982.
(11) Gérard, A.; Woolfe, A.; Mottet, G.; Reichen, M.; Castrillon, C.; Menrath, V.; Ellouze, S.; Poitou, A.; Doineau, R.; Briseno-Roa, L.; Canales-Herrerias, P.; Mary, P.; Rose, G.; Ortega, C.; Delincé, M.; Essono, S.; Jia, B.; Iannascoli, B.; Richard-Le Goff, O.; Kumar, R.; Stewart, S. N.; Pousse, Y.; Shen, B. Q.; Grosselin, K.; Saudemont, B.; Sautel-Caillé, A.; Godina, A.; McNamara, S.; Eyer, K.; Millot, G. A.; Baudry, J.; England, P.; Nizak, C.; Jensen, A.; Griffiths, A. D.; Bruhns, P.; Brenan, C. *Nat. Biotechnol.* **2020**, *38*, 715−721.
(12) Van Lent, J.; Breukers, J.; Ven, K.; Ampofo, L.; Horta, S.; Pollet, F.; Imbrechts, M.; Geukens, N.; Vanhoorelbeke, K.; Declerck, P.; Lammertyn, J. *Lab Chip* **2021**, *21*, 3627−3654.
(13) Sart, S.; Ronteix, G.; Jain, S.; Amselem, G.; Baroud, C. N. *Chem. Rev.* **2022**, *122*, 7061−7096.
(14) Zhao, L. X.; Sun, L.; Chu, X. G. *TrAC, Trends Anal. Chem.* **2009**, *28*, 404−415.
(15) Yang, M. W.; Huang, J. G.; Fan, J. L.; Du, J. J.; Pu, K. Y.; Peng, X. J. *Chem. Soc. Rev.* **2020**, *49*, 6800−6815.
(16) Xiao, Q.; Xu, C. X. *TrAC, Trends Anal. Chem.* **2020**, *124*, 115780.
(17) Yamanishi, C. D.; Chiu, J. H. C.; Takayama, S. *Bioanalysis* **2015**, *7*, 1545−1556.
(18) Ni, Y.; Arts, R.; Merkx, M. *ACS Sens.* **2019**, *4*, 20−25.
(19) Zhou, L. L.; Zhang, L. L.; Yang, L.; Ni, W.; Li, Y.; Wu, Y. H. *Biosens. Bioelectron.* **2021**, *173*, 112824.
(20) McConnell, E. M.; Cozma, I.; Mou, Q. B.; Brennan, J. D.; Lu, Y.; Li, Y. F. *Chem. Soc. Rev.* **2021**, *50*, 8954−8994.
(21) Xu, J. Q.; Jiang, R. D.; He, H. L.; Ma, C. B.; Tang, Z. W. *TrAC, Trends Anal. Chem.* **2021**, *139*, 116257.
(22) Zhang, R.; Wu, J.; Ao, H.; Fu, J. L.; Qiao, B.; Wu, Q.; Ju, H. X. *Anal. Chem.* **2021**, *93*, 9933−9938.
(23) Ao, H.; Xiao, W. C.; Chen, Y. H.; Wu, J.; Ju, H. X. *Sens. Actuators, B* **2023**, *383*, 133579.
(24) Golnak, R.; Xiao, J.; Atak, K.; Khan, M.; Suljoti, E.; Aziz, E. F. *J. Phys. Chem. B* **2015**, *119*, 3058−3062.
(25) Alsharabasy, A. M.; Pandit, A.; Farràs, P. *Adv. Mater.* **2021**, *33*, 2003883.
(26) Wang, Q. B.; Xu, N.; Gui, Z.; Lei, J. P.; Ju, H. X.; Yan, F. *Chem. Commun.* **2014**, *50*, 15362−15365.
(27) Wang, Q. B.; Xu, N.; Gui, Z.; Lei, J. P.; Ju, H. X.; Yan, F. *Analyst* **2015**, *140*, 6532−6537.
(28) Li, J.; Wu, H. P.; Yan, Y. R.; Yuan, T. X.; Shu, Y.; Gao, X.; Zhang, L.; Li, S. Q.; Ding, S. J.; Cheng, W. *Nucleic Acids Res.* **2021**, *49*, 13031−13044.
(29) Zheng, T.; Nie, W.; Yu, L.; Shu, J.; Li, Y.; Tian, C.; Wang, W.; Cui, H. *Proc. Natl. Acad. Sci. U.S.A.* **2022**, *119*, No. e2207693119.
(30) Pasternack, R. F. *Chirality* **2003**, *15*, 329−332.
(31) Szumilak, M.; Merecz, A.; Strek, M.; Stanczak, A.; Inglot, T. W.; Karwowski, B. T. *Int. J. Mol. Sci.* **2016**, *17*, 1560.
(32) Xu, J.; Wu, J.; Zong, C.; Ju, H. X.; Yan, F. *Anal. Chem.* **2013**, *85*, 3374−3379.
(33) Ghahremani Nasab, M.; Hassani, L.; Mohammadi Nejad, S.; Norouzi, D. *J. Biol. Phys.* **2017**, *43*, 5−14.
(34) Johnson, K. A.; Goody, R. S. *Biochemistry* **2011**, *50*, 8264−8269.
(35) Chen, J. L.; Zhang, Y. Y.; Cheng, M. P.; Guo, Y. H.; Sponer, J.; Monchaud, D.; Mergny, J. L.; Ju, H. X.; Zhou, J. *ACS Catal.* **2018**, *8*, 11352−11361.
(36) Mahshid, S. S.; Camiré, S.; Ricci, F.; Vallée-Bélisle, A. *J. Am. Chem. Soc.* **2015**, *137*, 15596−15599.
(37) Mahshid, S. S.; Vallée-Bélisle, A.; Kelley, S. O. *Anal. Chem.* **2017**, *89*, 9751−9757.
(38) Mahshid, S. S.; Mahshid, S.; Vallée-Bélisle, A.; Kelley, S. O. *Anal. Chem.* **2019**, *91*, 4943−4947.
(39) Peng, Y.; Li, X.; Yuan, R.; Xiang, Y. *Chem. Commun.* **2016**, *52*, 12586−12589.
(40) Porchetta, A.; Ippodrino, R.; Marini, B.; Caruso, A.; Caccuri, F.; Ricci, F. *J. Am. Chem. Soc.* **2018**, *140*, 947−953.
(41) Ranallo, S.; Sorrentino, D.; Ricci, F. *Nat. Commun.* **2019**, *10*, 5509.
(42) Zhang, M. X.; Zou, Y.; Xu, X.; Zhang, X. B.; Gao, M. X.; Song, J.; Huang, P. F.; Chen, Q.; Zhu, Z.; Lin, W.; Zare, R. N.; Yang, C. Y. *Nat. Commun.* **2020**, *11*, 2118.
(43) Wang, N. N.; Ao, H.; Xiao, W. C.; Chen, W. W.; Li, G. M.; Wu, J.; Ju, H. X. *Biosens. Bioelectron.* **2022**, *201*, 113959.
(44) Gao, Y. F.; Wang, Y. P.; He, B. S.; Pan, Y. C.; Zhou, D. T.; Xiong, M. Q.; Song, Y. J. *Angew. Chem., Int. Ed.* **2023**, *62*, No. e202302000.

https://doi.org/10.1021/acs.analchem.4c04122
Anal. Chem. 2024, 96, 18502−18509